

Quantitative CD3 PET Imaging Predicts Tumor Growth Response to Anti-CTLA-4 Therapy

Benjamin M. Larimer, Eric Wehrenberg-Klee, Alexander Caraballo, Umar Mahmood

Affiliation: Athinoula A. Martinos Center for Biomedical Imaging, Department of Radiology, Massachusetts General Hospital, Boston, MA, USA

Running Title: CD3 PET Predicts Immune Therapy Response

Keywords: CD3, PET, cancer immunotherapy, response prediction

Funding: P50-CA127003

*Correspondence to:

Umar Mahmood, M.D., Ph.D.
Athinoula A. Martinos Center for Biomedical Imaging
Department of Radiology
Massachusetts General Hospital
Boston, MA
Tel: 617-726-6477
Email: umahmood@mgh.harvard.edu

Benjamin Larimer, Ph.D.
Postdoctoral Fellow
Athinoula A. Martinos Center for Biomedical Imaging
Department of Radiology
149 13th Street, Charlestown, MA 02129
Tel: 617-726-6477
Email: blarimer@mgh.harvard.edu

Conflicts of Interest: None

Word Count: 3140 words

Figures: 4

ABSTRACT

Immune checkpoint inhibitors have made rapid advances, resulting in multiple Food and Drug Administration (FDA)-approved therapeutics that have markedly improved survival. However these benefits are limited to a minority sub-population that achieves a response. Predicting which patients are most likely to benefit would be valuable for individual therapy optimization. T cell markers such as CD3 represent a more direct approach than pre-treatment biopsy or genetic screening to monitoring tumor immune response, by directly examining active recruitment of T cells responsible for cancer cell-death. This approach could be especially effective as numerous different therapeutic strategies emerge, decreasing the need for drug-specific biomarkers and instead focusing on T cell infiltration, which has been previously correlated with treatment response. A CD3 positron emission tomography (PET) imaging agent targeting T cells was synthesized to test the role of such imaging as a predictive marker. The ^{89}Zr - p-isothiocyanatobenzyl-deferoxamine (DFO)-CD3 PET probe was assessed in a murine tumor xenograft model of colon cancer anti-cytotoxic T lymphocyte antigen-4 (CTLA-4) immunotherapy. Imaging on day 14 revealed two distinct groups of mice, stratified by PET signal intensity. Although there was no statistical difference in tumor volume on the day of imaging, in the high PET uptake group subsequent measurements revealed significantly smaller tumors than both the low-CD3 PET uptake group and untreated control. In contrast, low-CD3 PET uptake and untreated control mice demonstrated no statistical difference in size. These findings indicate that high-CD3 PET uptake in the anti-CTLA-4 treated mice is correlated with subsequent reduced tumor volume, and is a predictive biomarker of response.

INTRODUCTION

Rapid advances in the field of tumor immunology have led to multiple new therapies aimed at increasing the tumoral immune response against highly malignant cancers, with current approvals for treatment of melanoma, lung, and renal tumors, and multiple additional research programs ongoing (1-3). Response rates to these therapies are significantly higher than to standard chemotherapy (19-50% vs. 4-15%), and those that respond typically have more durable responses than with standard treatment (2,4,5). However, the majority of patients receiving immunotherapy will not respond, yet remain at risk of severe side-effects, which occur in up to 55% of patients (5). As of yet there remains no standard for identifying or predicting tumor response. Furthermore, evaluation of response to immunotherapies using standard imaging techniques remains challenging due to immune infiltrates that can masquerade as tumor growth (6). The desire to more rapidly identify patients likely to respond has spurred effort to elucidate both predictive biomarkers and also methods to better monitor therapeutic efficacy.

Significant evidence has accumulated to suggest that an increased presence of tumor infiltrating lymphocytes including CD4 and CD8 lymphocytes, is predictive of prognosis and response to immunomodulatory therapy (7-10). CD3 is a part of the T-cell receptor complex that serves as a global T lymphocyte marker and has also been correlated with response. By serving as a marker of total T cell infiltration, CD3 may represent a more abundant target than subpopulation markers, increasing PET signal and thus providing a more robust predictive marker.

Although tumor characterization is often accomplished through invasive biopsy, the highly heterogeneous and dynamic nature of the tumoral immune response limits the utility of this technology, and there is currently no established method to monitor CD3+ infiltrate. In

contrast, PET imaging of CD3 may provide an accurate and quantitative assessment of lymphocyte infiltrate across the entire tumor burden, including metastases, as well as normal organs, in real-time, without the need for repeated invasive procedures, and thus help to monitor and guide therapy. As such, we developed a CD3 PET probe to assess the ability of PET imaging to predict immune response to CTLA-4 checkpoint inhibitor therapy, which is being actively investigated in multiple clinical trials (e.g. NCT01975831, NCT02261220, NCT02060188, NCT02205333, among numerous others). A CD3-targeted antibody was conjugated to DFO and radiolabeled with ^{89}Zr with high purity and specificity. Conjugation and radiolabeling did not affect the ability of the probe to target CD3. The probe was used to quantitatively image CD3+ T cell infiltration in a murine model of colon cancer treated with an anti-CTLA-4 antibody, and to correlate imaging findings with *ex vivo* analysis. Quantitative PET imaging revealed a distinct difference in uptake between subsequent therapeutic responders and non-responders. CD3 PET imaging may represent a useful non-invasive imaging paradigm for predicting response to targeted immunotherapy prior to anatomical changes becoming apparent.

MATERIALS AND METHODS

Materials

All chemicals and liquid solvents were obtained from Sigma-Aldrich (St. Louis, MO) unless otherwise stated. CT-26 murine colon carcinoma cells and CD3-expressing murine T-cell lymphoma TK-1 cells were purchased from American Type Culture Collection (Manassas, VA) and cultured in RPMI-1640 media supplemented with 10% fetal bovine serum and 1% penicillin and streptomycin.

Antibody Conjugation and Radiolabeling

The monoclonal anti-mouse CD3 antibody clone 17A2 was purchased from R&D Systems (Minneapolis, MN). The antibody was reconstituted in sterile PBS and purified by size exclusion chromatography to ensure absence of impurities and dialyzed into 0.1M sodium bicarbonate, pH 9. Following purification, the antibody was conjugated to a bifunctional metal chelator by established protocols (11). Briefly, the antibody was diluted to 2 mg/mL in sodium bicarbonate buffer and mixed with 5 μ L of (3mg/mL) DFO (Macrocyclics, Dallas, TX) and incubated at 37°C for 30 min. The reaction was purified and buffer exchanged into 0.5M HEPES at a concentration of 1 mg/mL.

For radiolabeling, 74 MBq of ⁸⁹Zr-zirconium-oxalic acid (PerkinElmer, Waltham, MA) was adjusted to pH 7.2 with 1M sodium bicarbonate pH 9 and added to 0.5 mg of the DFO-CD3 antibody. The reaction was incubated for 1 h at room temperature, and unreacted ⁸⁹Zr was removed by size exclusion chromatography. The radiochemical purity was determined by instant thin layer chromatography and yield was determined by gamma-counter.

In Vitro ⁸⁹Zr-DFO-CD3 Binding Assays

In order to assess the affinity and specificity of the ⁸⁹Zr-DFO-CD3 antibody, a competitive binding assay was performed. The radiolabeled, purified antibody was diluted to 1x10⁶ CPM/mL in RPMI-1640 with 1% (w:v) bovine serum albumin and 10 μ L was added to 10⁵ CD3-expressing TK-1 murine lymphoma cells. As an antibody control, ⁸⁹Zr-DFO-Mouse IgG was also subjected to competitive binding analysis. Increasing amounts of unmodified antibody were added to appropriate aliquots, and incubated at 37°C for 1 h. Following incubation, cells were pelleted by centrifugation, washed 3 times with PBS, and counted by gamma counter.

Additionally, the cell specificity of each antibody was analyzed using either target TK-1 cells or CT26 murine colon cancer cells. Purified ^{89}Zr -DFO-CD3 or ^{89}Zr -DFO-IgG was added to 10^5 TK-1 or CT-26 cells at a concentration of 0.37 MBq and incubated at 37°C for 1 h. In the same manner as the competitive binding assay, cells were washed and subjected to quantification by gamma counter.

Ex Vivo Tumor Analysis

Ex vivo studies were performed by sacrificing treated mice on day 14 post tumor inoculation. Tumors were excised and divided equally for western blot and immunohistochemical analysis. For western blotting, tumors were lysed in 1% sodium dodecyl sulfate and subjected to sodium dodecyl sulfate-polyacrylamide gel electrophoresis. Blots were transferred to nitrocellulose, blocked with 5% non-fat dry milk and probed with the appropriate antibodies. Antibodies were diluted in 1% non-fat dry milk with 0.1% (v:v) Tween-20 as follows: CD3 (Abcam 16669, Cambridge, MA) 1:200, CD8 (Abcam108292) 1:1000, FoxP3 (Cell Signaling Technologies 4275S, Danvers, MA) 1:1000, and beta-actin (Cell Signaling Technologies 4970S) 1:1000. All primary antibody binding was detected by goat-anti rabbit-HRP conjugated antibody (Abcam ab6721) diluted at 1:1000 in the same buffer as the primary antibodies. Bands were detected by the addition of SignalFire™ ECL reagent (Cell Signaling Technologies) and visualized on a Kodak *in vivo* FX Pro system (Carestream Health, Rochester, NY) and semi-quantitative analysis performed using Carestream spectral imaging software. Immunohistochemistry was performed on formalin fixed, paraffin-embedded 10 micron slices of tumor. Antigen retrieval was performed using the microwave procedure with ethylenediaminetetraacetic acid buffer, pH 8. Anti-CD3 antibody (Abcam ab5690) was diluted at

1:200 and detected using a rabbit specific horseradish peroxidase/3,3'-diaminobenzidine detection immunohistochemistry kit (Abcam).

Anti-CTLA-4 Tumor Xenograft Treatment and Growth Curves

All animal studies were conducted with 8-12 week old female BALB/c mice (Charles River Laboratories (Wilmington, MA). Mice were housed and maintained by the Center for Comparative Medicine at Massachusetts General Hospital following animal protocols approved by the Institutional Animal Care and Use Committee. Tumor implantation was performed by injecting 5×10^5 CT26 cells diluted 1:1 in Matrigel (Corning, Waltham, MA) subcutaneously into the rear left flank. For immunomodulatory therapy studies, mice were treated with intraperitoneal injection of either 200 ng murine anti-CTLA-4 (n=7) (BioXCell, West Lebanon, NH) or normal saline (n=4) as a control. Mice were treated 4, 7 and 10 days following implantation of xenografts (10). Tumor sizes were monitored by caliper on days 7, 10, 12, 14 and 17 following inoculation.

Positron Emission Tomography Imaging

All PET imaging was performed using CT26 inoculated BALB/c mice treated according to the previously described therapeutic protocol. ^{89}Zr -DFO-CD3 was prepared as described, and an injected dose of 37 MBq/mL in normal saline was prepared. Tumor-bearing mice were injected on day 11, and the radiolabeled antibody was allowed to clear for 3 days. On day 14, mice were imaged on a rodent Triumph PET/computed tomography (CT) (GE Healthcare, Wilmington, MA). Following CT acquisition, PET images were obtained for 15 min in 2 bed positions. Images were constructed using 3D-MLEM (4 iterations, 16 subsets) and corrected for scatter and randoms. The mean standard uptake value (SUV_{mean}) for each tumor was calculated in a 3D region of interest auto-drawn around the tumor using a 30% isocontour threshold. A

region of interest surrounding the liver was also drawn to correct for injection efficiency and the tumor to liver ratio was calculated where $\text{tumor:liver SUV}_{\text{mean}} = \text{Tumor SUV}_{\text{mean}}/\text{Liver SUV}_{\text{mean}}$. Images were post-processed using VivoQuant (InviCRO, Boston, MA).

Statistical Analysis

Statistical analysis was performed using the Graphpad Prism Version 4 software. A non-linear regression was fit to competitive binding analysis and a two-way Student's t test was used to compare binding of ^{89}Zr -DFO-CD3 to TK-1 and CT26 cells and radiolabeled CD3 and IgG antibodies to TK-1 cells. Mean tumor volumes on day 17 were analyzed by one-way ANOVA and SUV_{mean} tumor:liver ratios were analyzed by unpaired t test. All quantifications represent the mean \pm SEM.

RESULTS

^{89}Zr -DFO-CD3 Radiolabeling and Binding Assays

A radiolabeled CD3-binding antibody was designed to analyze the infiltration of CD3+ cells into the tumor microenvironment following immunomodulatory therapy. To accomplish this, anti-CD3 antibody was conjugated with DFO, resulting in 0.8 ± 0.2 chelates per antibody, and labeled with the radioisotope ^{89}Zr (Fig. 1A). Average yield of radiolabeling was $68\pm 6\%$ with a specific activity of 50 ± 7 MBq/mg and radiochemical purity greater than 95%. Competitive binding analyses using both CD3 and control radiolabeled antibodies were performed and the results demonstrated the ^{89}Zr -CD3 PET probe bound with high affinity (2.6 ± 1.2 nM) and specificity to the CD3-expressing mouse lymphoma cell line (Fig. 1B). Cell binding with CD3-positive TK-1 cells and CD3-negative CT26 cells was assessed by measuring the retained counts per minute (CPM), which is directly correlated to total antibody binding. ^{89}Zr -DFO-CD3 had an

average of $47,700 \pm 4,080$ CPM binding, whereas ^{89}Zr -DFO-IgG resulted in only $6,430 \pm 495$ CPM ($P < 0.01$) (Fig. 1C). We also observed a significant difference in binding of the ^{89}Zr -CD3 probe between TK-1 ($47,700 \pm 4,070$ CPM) and CT26 cells ($4,550 \pm 445$ CPM; $P < 0.01$), confirming CD3-specific cell binding.

***Ex Vivo* Protein Expression Analysis of Anti-CTLA-4 Treated CT26 Tumor Xenografts**

Mice treated with anti-CTLA-4 therapy were sacrificed on day 14 post-inoculation, tumors excised, and biochemically analyzed. Initial whole-tumoral protein expression analysis by Western blot revealed distinct tumors with either high or low levels of CD3 (Fig. 2A). This trend remained unchanged when analyzing for CD8 expression as well. FoxP3, a marker of T_{Regs} was also analyzed and low FoxP3 expression was observed, indicating that CD3 was not correlated with an increased population of T_{Regs} (Fig. 2B). To confirm the cellular location of CD3 expression, IHC staining was utilized. CD3-high tumors revealed multiple areas of high-density CD3⁺ infiltrates, whereas a majority of the CD3-low tumor demonstrated no CD3 expressing cells (Fig. 2C).

Quantitative PET Imaging to Predict Tumor Growth Response to Anti-CTLA-4 Therapy

Following determination that conjugation and radiolabeling of the CD3 antibody resulted in a pure, highly specific probe for CD3-expressing cells and that immunomodulatory therapy resulted in an increase in CD3⁺ T cell infiltration, the ability to predict response to anti-CTLA-4 therapy was assessed (10). Subcutaneously injected xenograft tumors were readily visualized by PET imaging (Figs. 3A and 3B), revealing clear delineation of tumors, in addition to liver, spleen, lymph node and thymus uptake. Liver uptake is a well-known route of clearance for antibodies, and all other organs with accumulation are immune-related reservoirs of CD3⁺ T

cells (Fig. 3C). Tumor:liver SUV_{mean} ratios, which controlled for injection efficiency, revealed two distinct groups of mice, stratified by tumor uptake (Fig. 3D). The high tumor:liver group (n=3) demonstrated a tumor:liver ratio SUV range of 0.31-0.63 and mean of 0.48 ± 0.09 . The low tumor:liver group (n=4) demonstrated an tumor:liver ratio SUV range of 0.13-0.26 and mean of 0.19 ± 0.04 , a statistically significant comparison ($P < 0.05$).

Tumoral growth analysis

On day 14, the average tumor volume of the high-uptake group was $125 \pm 59 \text{ mm}^3$ (range = 34-234 mm^3) and the low-uptake average tumor volume was $41 \pm 10 \text{ mm}^3$ (range = 12-56 mm^3 , ($P = 0.35$)) (Fig. 4A). Vehicle-treated control mice (n=4) had a mean tumor volume of $167 \pm 30 \text{ mm}^3$ (range 100-245 mm^3), which was not statistically different than the high-uptake group ($P = 0.12$). Tumoral growth measurement on day 17 demonstrated a reversal of average tumor volumes, with the high PET uptake group measuring a significantly smaller tumor volume ($149 \pm 31 \text{ mm}^3$) than the low PET uptake ($433 \pm 42 \text{ mm}^3$; $P < 0.05$) and control groups ($519 \pm 102 \text{ mm}^3$; $P < 0.05$) (Fig. 4B).

DISCUSSION

Immune checkpoint inhibitors have made rapid advances over the previous decade. Three FDA-approved therapeutics, ipilimumab, pembrolizumab, and nivolumab have drastically improved overall survival in those patients who respond, however this is limited to a currently undefined subpopulation (2,12,13). A number of candidate biomarkers for response prediction, including PD-1, PD-L1, CD8 and CD3 are being analyzed through multiple methods, including biopsy, genetic screening, and molecular imaging (8,14,15). Although pre-therapeutic markers such as PD-L1 have been demonstrated to be partially predictive in specific cancers, less than

half of those who are determined to be PD-L1 positive achieve an objective response (16). Additionally, while next-generation sequencing has provided clues into the effects of mutational load on response to immune therapy, a definitive clinical mutational load has yet to be defined (17). In contrast, T cell markers such as CD3 represent a more direct approach to monitoring immune response to cancers by directly detecting active recruitment of T cells responsible for cancer cell death. This approach could be especially effective as numerous different therapeutic strategies emerge, eliminating the need for individual biomarkers and instead focusing on T cell infiltration as a common pathway for early assessment of therapeutic response. Although PET probes targeting PD-1 and CD8 have been investigated as imaging agents, correlation to immune response or tumor growth prior to tumor response divergence has not been demonstrated (18,19). Thus a CD3 imaging agent was sought to demonstrate not only the ability to image tumoral CD3 infiltration, but also to correlate with subsequent therapeutic response.

Following confirmation of specificity and affinity for CD3 expressing T cells, the ^{89}Zr -DFO-CD3 PET probe was tested in a murine tumor xenograft model of colon cancer immunotherapy, treating CT26 xenografts with either anti-CTLA-4 antibody or vehicle as a control. Analysis of CT26 tumors treated in this fashion had previously demonstrated differential CD3⁺ T cell infiltration, which was used as the basis for correlating differences in CD3 with survival. CD3 PET imaging on day 14 revealed two distinct groups of mice, one with high PET probe uptake versus the other with low uptake. Importantly, the tumor volumes of all mice on day 14 were not predictive of response, as the average tumor volume for the high uptake group was larger than the low PET uptake group, although the difference was not significant. By day 17 however, a clear response difference was observed, as the high PET uptake group tumor size remained significantly smaller than both the low PET uptake group and untreated control.

Furthermore, the low-CD3 PET uptake and untreated control mice demonstrated no statistical difference in size, and their large volume constituted an endpoint for the study. These findings indicate that high-CD3 PET uptake in the anti-CTLA-4 treated mice is correlated with immune response, and is a predictive biomarker of response.

Although the CD3 PET imaging data suggests a novel paradigm for predicting immune response in tumors treated with checkpoint inhibiting therapy, further work is required to validate and translate this paradigm for clinical application. Full-size IgG PET imaging has been successfully utilized in clinical imaging trials, but future work may benefit from pharmacokinetic optimization using smaller vectors such as peptides, small molecules or other smaller biologic constructs (e.g. scFvs, minibodies, affibodies or single domain V_HHs) in order to optimize injection to imaging time and improve specific uptake (19,20). Furthermore, the paradigm should be further evaluated with the myriad of immunotherapies currently under investigation, including vaccines, adoptive cell transfer, and combination therapies in other clinically relevant cancers such as lung and metastatic melanoma.

Immuno-oncology has greatly improved the outlook for patients otherwise facing a dim prognosis. This success has been tempered by the lack of clear indication as to who will respond to novel therapies. The results presented here demonstrate that imaging of CD3⁺ T cell infiltration is predictive of anti-CTLA-4 therapy tumor response, providing evidence that PET imaging can be used to predict therapeutic response.

REFERENCES

1. Callahan MK, Flaherty CR, Postow MA. Checkpoint blockade for the treatment of advanced melanoma. *Cancer Treat Res*. 2016;167:231-250.
2. Borghaei H, Paz-Ares L, Horn L, et al. Nivolumab versus Docetaxel in advanced nonsquamous non-small-cell lung cancer. *N Engl J Med*. 2015;373:1627-1639.
3. Motzer RJ, Escudier B, McDermott DF, et al. Nivolumab versus Everolimus in advanced renal-cell carcinoma. *N Engl J Med*. 2015;373:1803-1813.
4. Postow MA, Chesney J, Pavlick AC, et al. Nivolumab and Ipilimumab versus Ipilimumab in untreated melanoma. *N Engl J Med*. 2015;372:2006-2017.
5. Larkin J, Chiarion-Sileni V, Gonzalez R, et al. Combined Nivolumab and Ipilimumab or monotherapy in untreated melanoma. *N Engl J Med*. 2015;373:23-34.
6. Wolchok JD, Hoos A, O'Day S, et al. Guidelines for the Evaluation of Immune Therapy Activity in Solid Tumors: Immune-related response criteria. *Clin Cancer Res*. 2009;15:7412-7420.
7. Galon J, Costes A, Sanchez-Cabo F, et al. Type, density, and location of immune cells within human colorectal tumors predict clinical outcome. *Science*. 2006;313:1960-1964.
8. Pages F, Galon J, Dieu-Nosjean MC, Tartour E, Sautes-Fridman C, Fridman WH. Immune infiltration in human tumors: a prognostic factor that should not be ignored. *Oncogene*. 2010;29:1093-1102.
9. Tumei PC, Harview CL, Yearley JH, et al. PD-1 blockade induces responses by inhibiting adaptive immune resistance. *Nature*. 2014;515:568-571.
10. Duraiswamy J, Kaluza KM, Freeman GJ, Coukos G. Dual blockade of PD-1 and CTLA-4 combined with tumor vaccine effectively restores T-cell rejection function in tumors. *Cancer Res*. 2013;73:3591-3603.
11. Vosjan MJ, Perk LR, Visser GW, et al. Conjugation and radiolabeling of monoclonal antibodies with zirconium-89 for PET imaging using the bifunctional chelate p-isothiocyanatobenzyl-desferrioxamine. *Nat protoc*. 2010;5:739-743.
12. Herbst RS, Baas P, Kim D-W, et al. Pembrolizumab versus docetaxel for previously treated, PD-L1-positive, advanced non-small-cell lung cancer (KEYNOTE-010): a randomised controlled trial. *The Lancet*. December 19, 2015 [Epub ahead of print].

- 13.** Hodi FS, O'Day SJ, McDermott DF, et al. Improved survival with Ipilimumab in patients with metastatic melanoma. *N Engl J Med.* 2010;363:711-723.
- 14.** Ascierto PA, Kalos M, Schaer DA, Callahan MK, Wolchok JD. Biomarkers for immunostimulatory monoclonal antibodies in combination strategies for melanoma and other tumor types. *Clin Cancer Res.* 2013;19:1009-1020.
- 15.** Roxburgh C, McMillan D. The role of the in situ local inflammatory response in predicting recurrence and survival in patients with primary operable colorectal cancer. *Cancer Treat Rev.* 2012;38:451-466.
- 16.** Garon EB, Rizvi NA, Hui R, et al. Pembrolizumab for the treatment of non–small-cell lung cancer. *N Engl J Med.* 2015;372:2018-2028.
- 17.** Rizvi NA, Hellmann MD, Snyder A, et al. Mutational landscape determines sensitivity to PD-1 blockade in non–small cell lung cancer. *Science.* 2015;348:124-128.
- 18.** Maute RL, Gordon SR, Mayer AT, et al. Engineering high-affinity PD-1 variants for optimized immunotherapy and immuno-PET imaging. *Proc Natl Acad Sci U S A.* 2015;112:E6506-E6514.
- 19.** Tavaré R, Escuin-Ordinas H, Mok S, et al. An effective immuno-PET imaging method to monitor CD8-dependent responses to immunotherapy. *Cancer Res.* 2016;76:73-82.
- 20.** Pandit-Taskar N, O'Donoghue JA, Beylertgil V, et al. 89Zr-huJ591 immuno-PET imaging in patients with advanced metastatic prostate cancer. *Eur J Nucl Med Mol Imaging.* 2014;41:2093-2105.

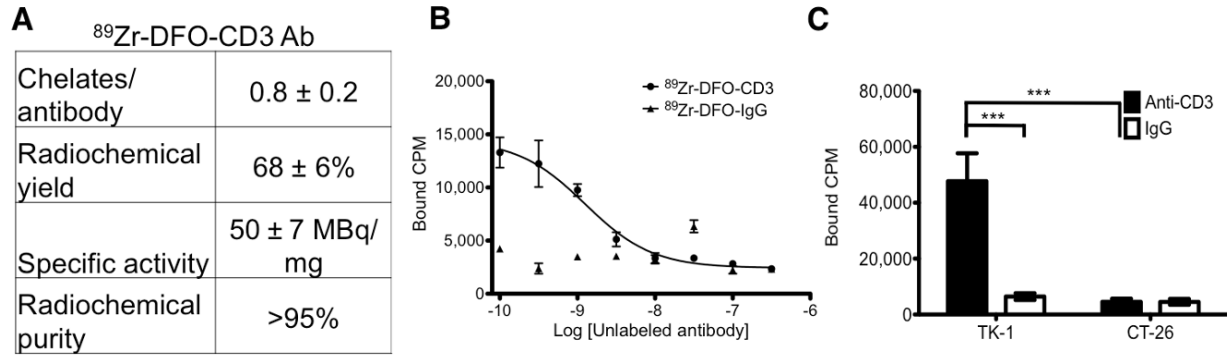


FIGURE 1 - ⁸⁹Zr-DFO-CD3 PET Imaging Antibody Characterization. A) Table describing synthesis and post-purification characteristics of the antibody B) Competitive binding assay using CD3+ mouse lymphoma cells and either radiolabeled CD3 antibody or control antibody. C) Cellular specificity of the CD3 probe and a control antibody was ascertained by cell binding assay with CD3+ TK-1 cells and CD3- CT26 murine colon carcinoma cells. *** - $P < 0.001$

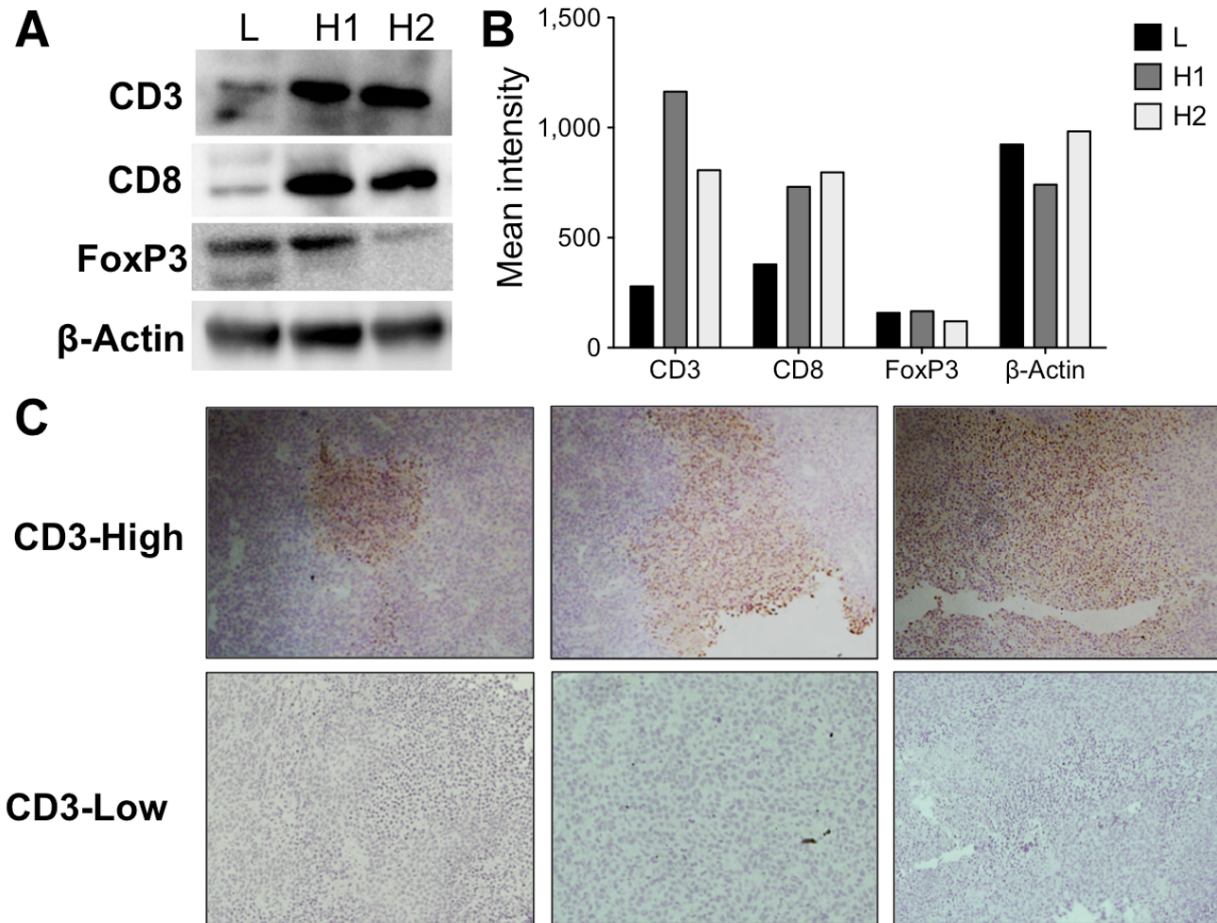


FIGURE 2 – *Ex Vivo* Tumor T Cell Infiltrate Protein Quantification and Localization A) Treated CT26 tumor tumors were excised 14 days post-inoculation. Western blot analysis revealed one low (L) CD3 expressing and two high (H) CD3 expressing tumors, which were also characterized for CD8, FoxP3 and β-actin. B) Quantification revealed relatively high concentrations of CD3 and CD8 in H tumors and uniformly low immunosuppressive FoxP3 protein. β-Actin analysis revealed similar overall total protein across all samples. C) Spatial localization of CD3 was detected using IHC. Representative areas of CD3 infiltration are shown for the CD3-high and CD3-low tumors.

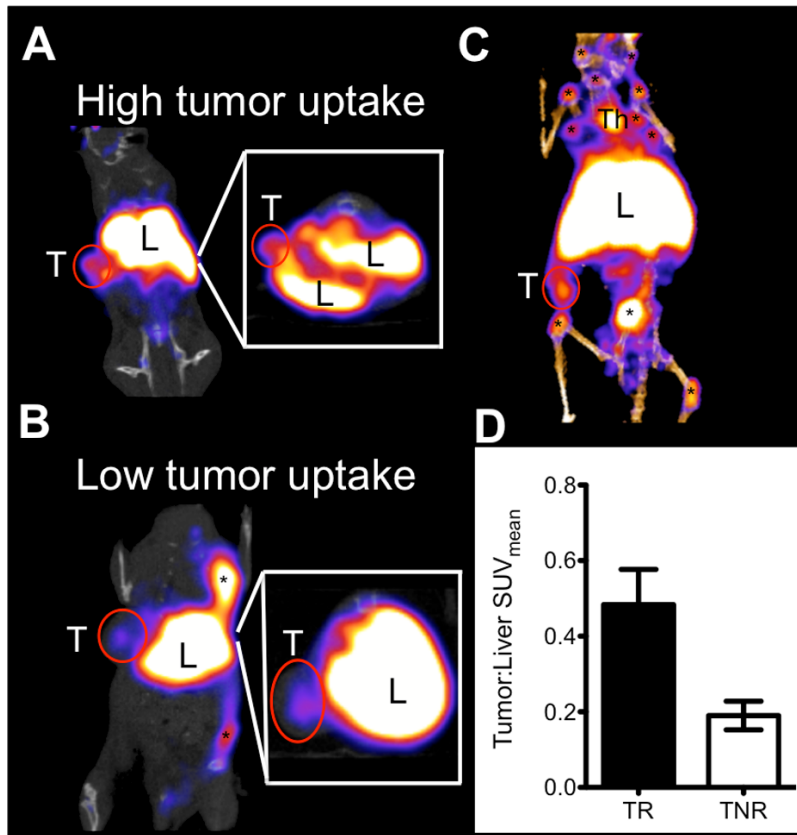


FIGURE 3 – PET Imaging of Anti-CTLA-4 Treated CT26 Tumor Bearing Mice. A) A representative coronal image of a high uptake mouse depicts high tumor uptake (White T), in addition to expected hepatobiliary clearance through the liver (L). The inset illustrates an axial slice through the tumor, with high tumor uptake in addition to uptake in two lobes of the liver. B) A coronal image of a low uptake mouse shows markedly lower tumor uptake in comparison to the high uptake mouse. Two lymph nodes, denoted by asterisks are also visible in the plane of view. An axial slice of the tumor is also shown to further illustrate uptake. C) A coronal image with clear visualization of tumor (T), liver (L) and lymph nodes (*). D) Quantification of PET SUV_{mean} tumor to liver ratios validates significant differences in uptake between the low and high groups. * = $P < 0.05$

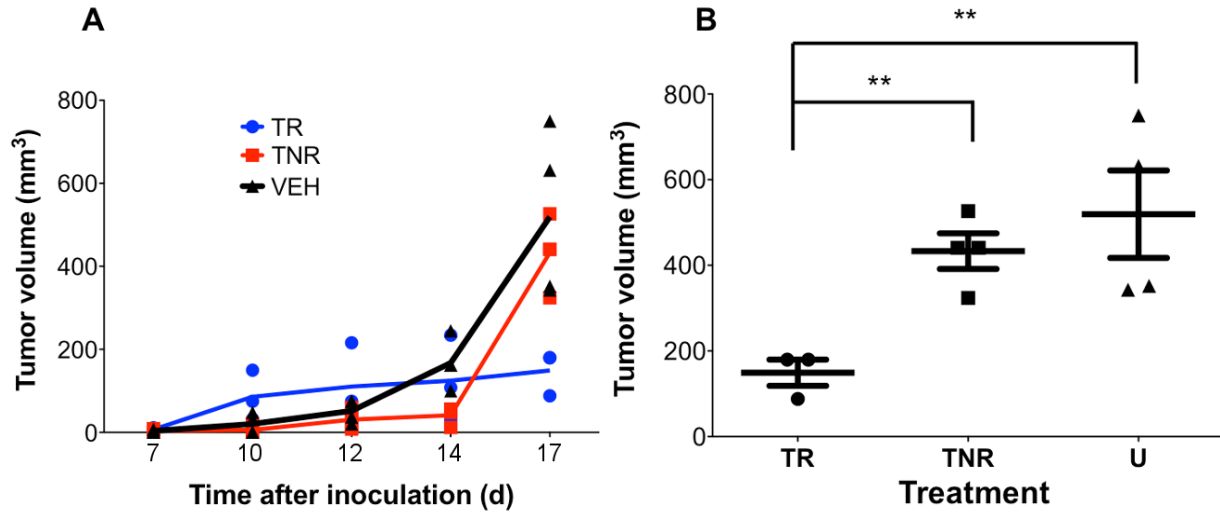


FIGURE 4 – Tumor Growth Curves and Day 17 Individual Tumor Analysis. A) The mean volumes of n=3-4 mice are plotted on each day of measurement \pm SEM. The blue curve represents treated responders (TR), the red curve represents treated non-responders (TNR) and the black curve represents vehicle treated mice. B) Individual tumor volumes from the treated responder (TR), treated non-responder (TNR) and vehicle (VEH) are shown on a scatter plot, with the error bars representing the SEM.